

Electrochemical and Infrared Spectroscopic Studies
Provide Insight into Reactions of the NiFe
Regulatory Hydrogenase from *Ralstonia eutropha*
with O₂ and CO

*Philip A. Ash,^a Juan Liu,^a Nathan Coutard,^a Nina Heidary,^b Marius Horch,^b Ingvild Gudim,^a
Thomas Simler,^a Ingo Zebger,^b Oliver Lenz,^{b*} Kylie A. Vincent^{a*}*

^a Department of Chemistry, University of Oxford, Inorganic Chemistry Laboratory, South Parks Road, Oxford, OX1 3QR.

^b Technische Universität Berlin, Institut für Chemie, PC14, Berlin, Germany

Email. kylie.vincent@chem.ox.ac.uk; oliver.lenz@tu-berlin.de

Abstract

The regulatory hydrogenase (RH) from *Ralstonia eutropha* acts as the H₂-sensing unit of a two-component system that regulates biosynthesis of the energy conserving hydrogenases of the organism according to the availability of H₂. The H₂ oxidation activity, which was so far determined *in vitro* with artificial electron acceptors, has been considered to be insensitive to O₂ and CO. It is assumed that the presence of bulky isoleucine and phenylalanine amino acid residues close to the NiFe active site ‘gate’ gas access, preventing molecules larger than H₂ interacting with the active site. We have carried out sensitive electrochemical measurements to demonstrate that O₂ is in fact an inhibitor of H₂ oxidation by the RH, and that both H⁺ reduction and H₂ oxidation are inhibited by CO. Furthermore we have demonstrated that the inhibitory effect of O₂ arises due to interaction of O₂ with the active site. Using protein film infrared electrochemistry (PFIRE) under H₂ oxidation conditions, in conjunction with solution infrared measurements, we have identified previously unreported oxidized inactive and catalytically active reduced states of the RH active site. These findings suggest that the RH has a rich active site chemistry similar to that of other NiFe hydrogenases.

Keywords

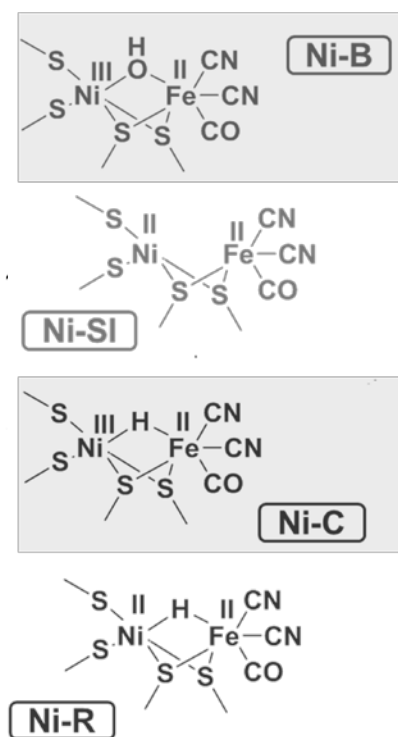
Infrared spectroelectrochemistry; enzyme inhibition; protein film electrochemistry; gas access; biological hydrogen cycling

Introduction

A nickel-iron catalytic site, incorporating iron coordinated by biologically unusual CO and CN⁻ ligands, is common to hydrogenases having various biological roles. The Ni is linked to Fe^{II} via two bridging cysteine thiolates in addition to coordination by two terminal cysteine ligands.¹ During catalysis the Ni cycles through formal oxidation states of III and II,¹ and there is growing evidence for involvement of a Ni^I intermediate.²⁻⁴ The Knallgas bacterium *Ralstonia (R.) eutropha* possesses four NiFe hydrogenases which allow cells to grow on H₂ as the sole energy source with O₂ as a terminal electron acceptor.⁵⁻⁶ Energy from H₂ is extracted and stored by the periplasmically oriented membrane bound hydrogenase (MBH),⁷ a cytoplasmic NAD⁺-linked soluble hydrogenase (SH)⁸ and an actinobacterial-type hydrogenase (AH).⁶ Synthesis of these enzymes is controlled at the transcriptional level by a H₂-sensing system involving a regulatory Ni-Fe hydrogenase (RH), a histidine protein kinase and a response regulator.⁹ The regulatory hydrogenase is composed of the subunits HoxBC and occurs natively as a pair of HoxBC units that is associated with a histidine protein kinase tetramer.¹⁰⁻¹¹

Nickel-iron hydrogenases have differing levels of sensitivity to dioxygen. Exposure to O₂ usually leads to formation of oxidized inactive forms of the active site which can be re-activated by reduction.¹ One feature controlling the extent of hydrogenase activity retained in air is the relative rate of reaction with O₂ compared to re-activation of the hydrogenase.¹² The best characterized inactive oxidized state of NiFe hydrogenases is known as Ni-B, and incorporates a hydroxide ligand in the bridging position between Ni^{III} and Fe^{II} (Scheme 1).^{1, 13-14} Another inactive state at the same redox level, known as Ni-A, is differentiated from Ni-B on the basis of slower kinetics of reactivation.¹⁵

Scheme 1. Redox levels of the active site of NiFe hydrogenases. Paramagnetic states, detected by EPR spectroscopy, are shown on a gray background. Several forms of the active site are known at each redox level. For the RH, only the Ni-SI and Ni-C levels have been assigned previously using infrared spectroscopy.



Aerobic growth of *R. eutropha* on H_2 and O_2 necessitates its hydrogenases having a high degree of tolerance to O_2 , and different mechanisms for this have been described for the MBH¹⁶ and SH.¹⁷⁻¹⁹ The RH has been denoted insensitive to O_2 and CO on the basis that biochemical H_2 oxidation activity assays with methylene blue as artificial electron acceptor are not significantly affected by the presence of O_2 or CO during H_2 turnover, and aerobically purified samples have very similar activity to anaerobically purified samples.²⁰⁻²¹ Inactive states of the active site have so far not been detected spectroscopically for the native RH, although additional active site redox

states were evident in infrared spectra of variants with modifications to amino acids close to the active site.²² One clear difference between regulatory hydrogenases and the energy conserving NiFe hydrogenases is the presence of two bulky amino acids, isoleucine and phenylalanine, close to the active site in place of less bulky valine and leucine, respectively, which are found in most other hydrogenases.⁵ It has been suggested that the bulky amino acids restrict the access of gases larger than H₂ to the active site.²³ Site-directed mutations to replace either or both of the bulky isoleucine and phenylalanine residues in RH with valine and leucine, respectively, led to drastic drops in the H₂-mediated methylene blue reduction activity of enzyme samples purified in air, and anaerobically purified samples of these variants lost activity rapidly on exposure to air.²⁰ In the RH variant containing both replacements activity could be restored by reduction with dithionite, suggesting that inactive oxidized states were responsible for the loss of activity after O₂-exposure,²⁰ similar to ‘standard’ NiFe hydrogenases. These results suggest that the bulky residues in the native RH may confer some protection against O₂.

Carbon monoxide is well established as a reversible inhibitor of most NiFe hydrogenases, although a mild sensitivity (or even insensitivity) to CO is a trait that has been associated with the O₂-tolerant hydrogenases, including the MBH from *R. eutropha* and *Aquifex aeolicus* and Hydrogenase 1 from *Escherichia (E.) coli*.²⁴⁻²⁶ Since the CO molecule has a similar hydrodynamic radius to O₂, it is useful as a probe for what size of gaseous molecules can enter a hydrogenase.²⁶ Here we present results on RH, studied for the first time under direct electrochemical control, which confirm that that O₂ and CO can access the active site of RH and attenuate its catalytic activity.

Protein film electrochemistry (PFE) has been used widely in studying the catalysis and reactions of hydrogenases.^{15, 27-28} In this approach, the protein is immobilized on an electrode as a sub-

monolayer film, often by facile adsorption onto a graphitic carbon surface, and engages in direct electron transfer with the electrode. Electron exchange with the electrode is enabled by a relay chain of iron sulfur clusters, possessed by all NiFe hydrogenases, which connect the buried active site with the native electron acceptors. Rapid rotation of the electrode during a PFE experiment provides efficient mass transport of substrate to the electrode and product away from the electrode. In the presence of H_2 and at potentials more positive than $E(H^+/H_2)$ the electrode functions as the electron acceptor, and each cycle of H_2 oxidation by the enzyme leads to electron transfer to the electrode and is recorded as a positive current response. A highly active enzyme thus gives rise to a high catalytic current. Although NiFe hydrogenases function primarily in the H_2 oxidation direction under physiological conditions, reduction of protons to produce H_2 at potentials more negative than $E(H^+/H_2)$ is observed for most NiFe hydrogenases, although this reaction is typically inhibited fairly strongly by H_2 .¹⁵ The RH has a low H_2 oxidation turnover frequency ($2-5\text{ s}^{-1}$ measured with methylene blue as electron acceptor),²¹ and this may have discouraged its study previously by PFE. However we show here that the RH immobilized on a graphite electrode gives rise to clear electrocatalytic H_2 oxidation and H^+ reduction waves under a H_2 atmosphere. The current in PFE is very sensitive to changes in activity in response to potential or to the introduction of inhibitors, and we use this approach to study subtle effects of CO and O_2 on the activity of the RH. Additionally we exploit a new approach to infrared (IR) spectroscopy we have developed which combines the direct electrochemical control of PFE with attenuated total reflectance (ATR)-IR sampling of hydrogenase on a carbon electrode (PFIRE).⁴ This has allowed us to evaluate the effect of O_2 on the redox states of the RH active site under H_2 oxidation turnover conditions, complemented by

transmission IR measurements on the RH in solution to monitor aerobic oxidation of the active site.

Experimental

Protein preparation

Preparations of *R. eutropha* RH used for PFE and PFIRE measurements were a monomeric form of HoxBC with a Strep affinity tag to facilitate purification (RH_{stop}) which was purified according to a published procedure²⁰ and concentrated to 28.8 mg mL⁻¹. Transmission IR measurements were performed on wild type RH, purified as previously described.²⁹ Mixed buffer solution (pH 6, 15 mM) was prepared from MES, TAPS, CHES, Sodium Acetate (Sigma-Aldrich) and HEPES (Melford) with NaCl (100 mM, Fisher Scientific) as supporting electrolyte. Phosphate buffer (pH 6.0, 50 mM) was prepared from K₂HPO₄ (BDH) and KH₂PO₄ (Sigma) with KCl (100 mM, Fisher Scientific) as supporting electrolyte. Ultra high-purity water (18 MΩ cm, MilliQ, Millipore) was used throughout.

Protein film electrochemistry (PFE)

Electrochemical experiments were carried out in a N₂-filled anaerobic glove box (Mbraun, <1 ppm O₂) in a glass electrochemical cell, water-jacketed for temperature control by a water circulator (Grant), and sealed *via* an o-ring onto an electrode rotator (EG&G model 636). Gas inlet and outlet fittings allow exchange of gases in the headspace. The counter electrode was a platinum wire (Surepure Chemetals, 99.99 %, 26 gauge), and a saturated calomel reference electrode (SCE) was used. Electrochemical control was provided by an Autolab PGSTAT 128N, and potentials were converted to volts *vs* the standard hydrogen electrode (SHE) using the conversion $E_{\text{SHE}} = E_{\text{SCE}} + 241 \text{ mV}$ at 30 °C. The electrochemical cell was washed with *aqua*

regia between experiments and rinsed thoroughly with water. A homemade pyrolytic graphite ‘edge’ (PGE, Momentive Performance Materials) rotating disc electrode (RDE) with a surface area of 0.03 cm^2 was used as the working electrode. To ensure a fresh surface for RH adsorption the PGE working electrode was polished with a slurry of α -alumina ($1\text{ }\mu\text{m}$, Buehler) and rinsed by ultrasonication in water before application of approximately $0.5\text{ }\mu\text{L}$ of as-received RH_{stop} . The enzyme was allowed to adsorb for approximately 1 min, before rinsing with water to remove any unadsorbed RH_{stop} . The electrode was rotated for 30 seconds before starting an experiment to ensure that the solution was in equilibrium with the initial gas mixture. Gas mixtures were prepared using mass flow controllers (Brooks); H_2 , N_2 and CO gases were purified using an O_2 -removal filter (Varian Gas Clean Filter, gas outlet quality $<50\text{ ppb O}_2$). The RH is known to have a particularly low activity, and therefore capacitive current makes a significant contribution to the overall current observed. The capacitive contribution cannot easily be subtracted since the capacitance differs from one electrode preparation to another, and is generally significantly different for unmodified and enzyme-modified electrodes. Additional slow decay in current at electrodes modified with RH_{stop} is attributed to film loss, due to either RH desorption or potential-dependent damage throughout the experiment.

Protein film infrared electrochemistry (PFIRE)

To prepare enzyme-modified carbon particles, a $10\text{ }\mu\text{L}$ aliquot of as-purified RH_{stop} was transferred into a mixed buffer system at pH 6.0, containing no NaCl, by dilution and reconcentration using a 30kDa cut-off microcentrifugal concentrator (GE Healthcare). The desalted RH_{stop} was added to $5\text{ }\mu\text{L}$ of a dispersion of carbon black particles in water (20 mg mL^{-1} , Black Pearls 2000, Cabot Corporation, used as received) and the mixture left at $1\text{ }^\circ\text{C}$ overnight to allow enzyme adsorption. Unadsorbed enzyme was then removed by washing with several

aliquots of mixed buffer. Enzyme adsorption was carried out in a N₂-filled glove box (<1 ppm O₂, Glove Box Technology Ltd).

Simultaneous IR and electrochemical measurements were carried out using a spectroelectrochemical ATR-IR technique, PFIRE, as previously described.⁴ Briefly, a 1 μ L aliquot of enzyme-modified particles was drop-cast onto a multiple-reflection Si internal reflection element (IRE, $8.39 \times 5 \times 1$ mm³, face angle of 39°, Crystal GmbH) sealed into a polyether ether ketone (PEEK) base. Lateral electronic connection was provided by a piece of carbon paper (Toray, TGP-H-030) placed on top of the deposited particles. The spectroelectrochemical cell body, also constructed from PEEK, was then sealed onto the base and filled with N₂-saturated buffered electrolyte. The spectroelectrochemical cell body houses a miniature saturated calomel reference electrode, prepared as previously described,⁴ a Pt wire counter electrode (Surepure Chemetals, 99.99 %, 26 gauge) and a carbon rod working electrode connection. An additional inlet and outlet allowed flow of fresh buffered electrolyte through the cell *via* a peristaltic pump (QL-1000, Williamson Pumps Ltd) at a flow rate of 25 mL minute⁻¹. Gas-saturated buffers were prepared by equilibrating the buffer with mixtures of H₂, N₂ and O₂. Gas mixtures were prepared at 1 bar using mass flow controllers (Brooks) and H₂ and N₂ were purified by passing through an O₂-removal filter (Restek Super-Clean, gas outlet quality >99.9999%). The Si IRE was cleaned by successive ultrasonication in sulphuric acid, nitric acid and water. Electrochemical control was provided by an Autolab PGSTAT 128N, and potentials were converted to volts *vs.* the standard hydrogen electrode (SHE) using the conversion $E_{\text{SHE}} = E_{\text{SCE}} + 241$ mV at 30 °C. Prior to experiments RH_{stop} was activated under 1 bar H₂ at -500 mV for 30 minutes. Infrared spectra were recorded using a Bruker Vertex 80 spectrometer equipped with a liquid nitrogen-cooled mercury cadmium telluride (MCT) detector and custom-modified

ATR accessory (GladiATR, Pike Technologies) and controlled by OPUS software. Spectra were recorded as the coaddition of 1024 interferograms collected at 2 cm^{-1} resolution. The spectrometer is housed inside an anaerobic, dry glove box ($<1\text{ ppm O}_2$, $<-94^\circ$ dew point, Glove Box Technology Ltd). Baseline correction was carried out in Origin 9.1, using 2nd derivative spectra to aid the identification of peak positions.

Transmission infrared spectroscopic measurements during gas exchange in the solution phase

IR transmission measurements of double dimeric wild type RH were carried out on a Bruker Tensor 27 spectrometer equipped with a liquid nitrogen-cooled photovoltaic MCT detector. Reduction of wild type RH was carried out in an anaerobic chamber (containing N_2 and up to 5% H_2) by incubating the enzyme under 1 bar H_2 for 30 min at room temperature. An aliquot (approximately $7\text{ }\mu\text{L}$) of the protein sample was injected into a temperature-controlled gas-tight transmission cell with CaF_2 windows (optical pathlength = $50\text{ }\mu\text{m}$). The temperature was set to $10\text{ }^\circ\text{C}$ by Peltier elements counter cooled by a thermostat. After recording a spectrum of the H_2 -reduced sample, air was allowed to slowly diffuse into the transmission cell inducing slow re-oxidation of the enzyme which was monitored spectroscopically. Spectra were recorded as the co-addition of 200 interferograms at a spectral resolution of 2 cm^{-1} . Baseline correction and spectral analysis were performed using Bruker OPUS software.

Results and Discussion

Electrocatalytic H₂ oxidation and H⁺ reduction by RH

Cyclic voltammograms recorded at a rotating disc electrode modified with RH_{stop} at pH 6.0 and 1 bar H₂ are presented in Figure 1 (red lines) and show clear electrocatalytic proton reduction (negative current) at low potentials, and H₂ oxidation at high potentials (positive current). During three consecutive voltammetric cycles the current response decreases by only 15% (measured at -0.6 V), showing that the RH is relatively stable on the electrode. A voltammogram recorded at an unmodified electrode under the same conditions (Figure 1, gray line) shows no electrocatalytic activity. The H⁺ reduction capacity of the RH is notable in comparison to other NiFe hydrogenases, and in particular the ‘O₂-tolerant’ enzymes, which tend to be biased toward H₂ oxidation with H⁺ reduction being inhibited by the product, H₂. The onset potentials for both H⁺ reduction and H₂ oxidation by the RH occur close to the thermodynamic potential for the 2H⁺/H₂ couple under these experimental conditions (-0.36 V, dashed vertical line) showing that the RH functions with no significant overpotential in either direction. This also contrasts with the behavior of NiFe hydrogenases which have been classed as ‘O₂ tolerant’, including *R. eutropha* and *Aquifex aeolicus* MBH enzymes and *E. coli*. Hydrogenase 1 for which a clear overpotential is observed before the onset of H₂ oxidation.^{24-25, 30} The current at the RH electrode is low for both electrocatalytic processes compared with that for most other NiFe hydrogenases studied by PFE,^{12, 15, 24, 28} in line with the known function of the RH as part of a cellular H₂-sensing system rather than an energy converting enzyme.

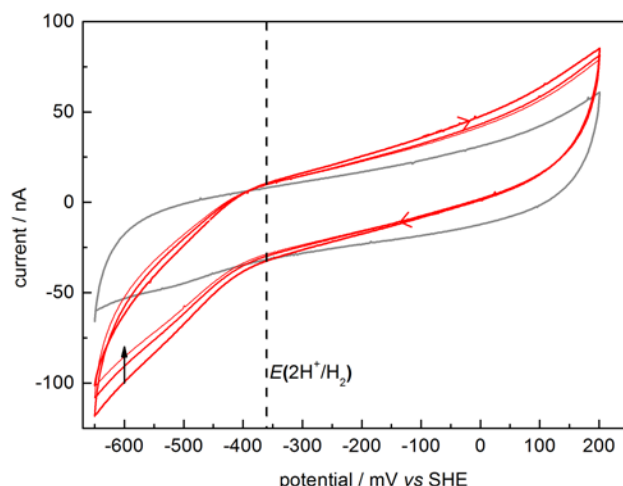


Figure 1. Cyclic voltammograms of a pyrolytic graphite ‘edge’ rotating disc electrode modified with RH_{stop} , recorded at pH 6.0 under 1 bar H_2 (red lines). Electrode rotation rate 2500 rpm; scan rate 10 mV s^{-1} ; temperature 30°C . A voltammogram recorded at an unmodified electrode under the same conditions (gray line) is also shown.

An electrochemical method was used to determine the Michaelis Menten constant, K_M , of the RH_{stop} for H_2 at $+150 \text{ mV}$ and 30°C , involving stepwise decreases in the mix of H_2 and N_2 in the headspace of the electrochemical cell from a starting level of 1 bar H_2 in the headspace, as shown in Figure 2. At the end of the experiment, the headspace gas was replaced with 1 bar H_2 to allow for correction for the loss in activity of the enzyme film during the course of the experiment. Analysis of this data using a Lineweaver Burk plot (Figure 2b) yielded a value of $K_M(\text{H}_2) = 15 \pm 3 \mu\text{M}$, close to values of $25 \pm 5 \mu\text{M}$ measured with methylene blue as electron acceptor (midpoint potential $+11 \text{ mV}$),²¹ and $5 \mu\text{M}$ with benzyl viologen (midpoint potential -374 mV),³¹ confirming that the enzyme retains normal sensitivity to H_2 when immobilized on the electrode. Electrochemical measurements were also conducted at -50 mV and $+50 \text{ mV}$ and we were unable

to detect any significant change in $K_M(\text{H}_2)$ at these potentials. The $K_M(\text{H}_2)$ for the RH is higher than that of *R. eutropha* MBH (6 μM),³² and similar to that of the SH³³ which may be important in allowing cells to avoid switching on hydrogenase gene expression in response to trace H_2 in their environment.

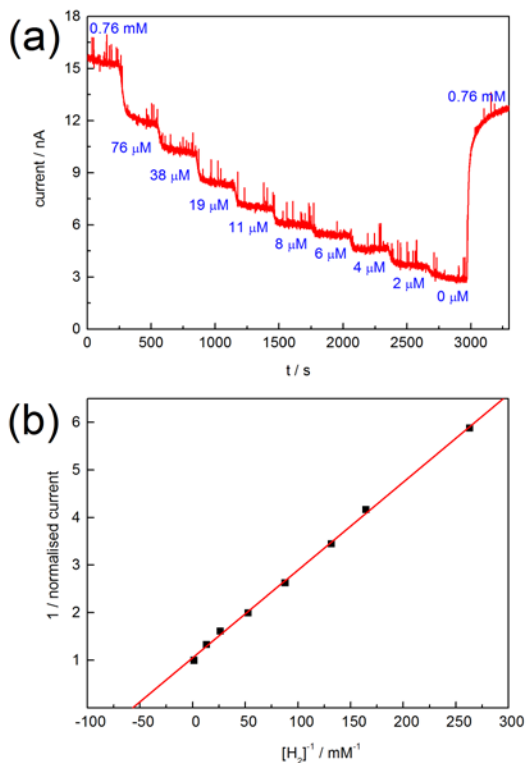


Figure 2. (a) Typical chronoamperometry experiment used to determine the K_M for H_2 by RH immobilized on a pyrolytic graphite rotating disc electrode. The H_2 oxidation activity (current) is monitored as a function of the content of H_2 in the headspace of the electrochemical cell; (b) Lineweaver Burk plot used to determine $K_M(\text{H}_2)$. The electrode was held at +150 mV throughout. Other conditions: pH 6, 30 °C and electrode rotation rate of 3300 rpm. The gas flushing through the headspace of the cell was maintained at an overall flow rate of 1 L min^{-1} .

CO is a weak inhibitor of H_2 oxidation by the RH

Electrochemical measurements provide a sensitive way to probe the effects of inhibitors because the current reports directly on enzyme activity. Figure 3 shows the result of a chronoamperometry experiment at +150 mV revealing the effect of CO on H_2 oxidation by the RH. The cell headspace was first flushed with a gas mixture comprising 90% N_2 , 10% H_2 . At 200 s, the gas mixture was exchanged for one comprising 90% CO, 10% H_2 , resulting in a drop in electrocatalytic current by about 15% (taking into account the background current measured under N_2 between 800-1000 s when there should be no electrocatalysis; this background current is attributed to small resistive contributions at the electrode). The H_2 oxidation current is restored when CO is flushed out of the cell, showing that CO is a mild and reversible inhibitor of H_2 oxidation by the RH.

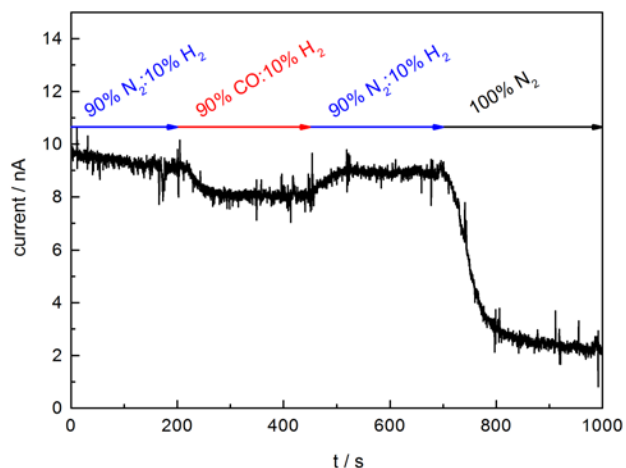


Figure 3. Current vs time trace for a pyrolytic graphite rotating disc electrode modified with RH_{stop} , showing the effect of CO on H_2 oxidation at +150 mV. Other conditions are: pH 6, 30 °C, electrode rotation rate: 4000 rpm. The headspace of the electrochemical cell was flushed with the gas mixtures indicated. The electrode was subjected to pre-equilibration at +150 mV.

CO and H₂ are weak inhibitors of H⁺ reduction by RH

Figure 4 shows the result of a chronoamperometry experiment at -500 mV to examine the effects of H₂ and CO on H⁺ reduction by the RH. For the first 350 s of the experiment, the headspace of the electrochemical cell was flushed with N₂. The difference in current between the trace for the enzyme-modified electrode and the corresponding trace for an unmodified electrode gives an indication of the level of electrocatalytic H⁺ reduction by the RH under an inert atmosphere at this potential, although it is not appropriate to subtract the current from the unmodified electrode trace since the background capacitive and resistive contributions to the current alter slightly upon modification of the graphite surface with the enzyme. The headspace gas in the cell was then exchanged for H₂, leading to a drop of ca 20% in the current magnitude. The current is restored when the head gas is returned to N₂, showing that H⁺ reduction is reversibly inhibited by H₂. It is difficult to quantify the extent of inhibition of H⁺ reduction by H₂ since the presence of H₂ causes a negative shift in the potential of the H⁺/H₂ couple which diminishes the thermodynamic driving force for H⁺ reduction at any given potential, and this is also expected to lead to a drop in electrocatalytic H⁺ reduction current. Exchange of the headspace gas by CO also results in a drop in the current magnitude, this time by about 45%, showing that CO is a more potent inhibitor of H⁺ reduction by RH than H₂, and inhibits H⁺ reduction by the RH more strongly than H₂ oxidation.

In other NiFe hydrogenases, CO is known to bind at the Ni atom of the active site,³⁴⁻³⁶ and to competitively inhibit H₂ oxidation.^{24, 37} The fact that CO reversibly inhibits both H₂ oxidation and H⁺ reduction by the RH thus suggests that gases larger than H₂ can reach the RH active site.

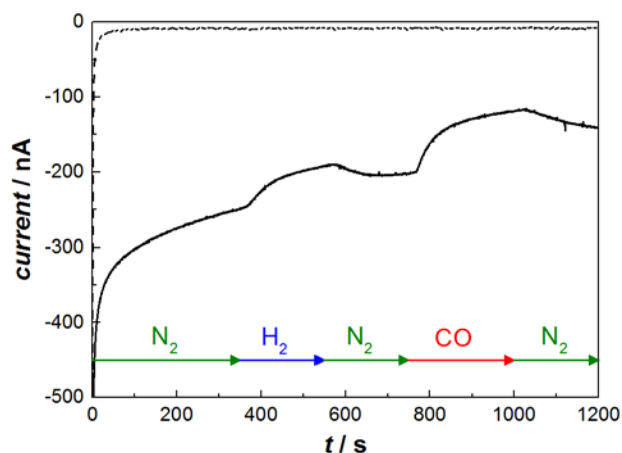


Figure 4. Current vs time trace for a pyrolytic graphite rotating disc electrode modified with RH_{stop} showing the effects of H_2 and CO on H^+ reduction by RH at -500 mV (solid line), together with the background current at an unmodified electrode (dotted). Other conditions are: pH 6, 30°C , electrode rotation rate of 3000 rpm. The headspace of the electrochemical cell was flushed with the gas mixtures indicated. The electrode was subjected to pre-equilibration at -500 mV for 100 s.

Dioxygen reversibly inactivates the RH at high potential

Figure 5 shows the effect of O_2 on electrocatalytic H_2 oxidation by the RH at $+200$ mV. The cell was first flushed with 98% H_2 , 2% N_2 . Keeping the H_2 concentration constant, 2% O_2 was then introduced into the headspace gas. This resulted in a clear decay in H_2 oxidation current over about 300 s, showing that at this potential, the RH is highly sensitive to O_2 . The current did not recover when O_2 was flushed out of the cell with 98% H_2 , 2% N_2 while the electrode remained poised at $+200$ mV, but H_2 oxidation activity at $+200$ mV was recovered by a series of low potential reactivation steps (-400 mV) of duration 1 s, 120 s and 300 s as shown in Figure 5. The

negative current during the re-activation steps is not shown in Figure 4 for clarity due to large capacitive effects. We were unable to measure the effect of O₂ on RH activity at lower potentials due to O₂ reduction at graphite which gives rise to a negative contribution to the current that complicates interpretation of the H₂ oxidation current arising from the enzyme.

Reactions of the MBH enzymes from *Aquifex aeolicus* and *R. eutropha* with O₂ have been studied in detail; although these enzymes have substantial O₂-tolerance at potentials close to $E(\text{H}^+/\text{H}_2)$, their sensitivity to O₂ increases as the potential is raised to more positive values where the rate of inactivation by O₂ becomes slow compared to the reactivation. For the RH, methylene blue-linked H₂ oxidation was not observed to be sensitive to prior aerobic incubation or to the presence of O₂ during H₂ turnover,^{21, 31} suggesting that the sensitivity to O₂ might also decrease as the potential becomes more negative.

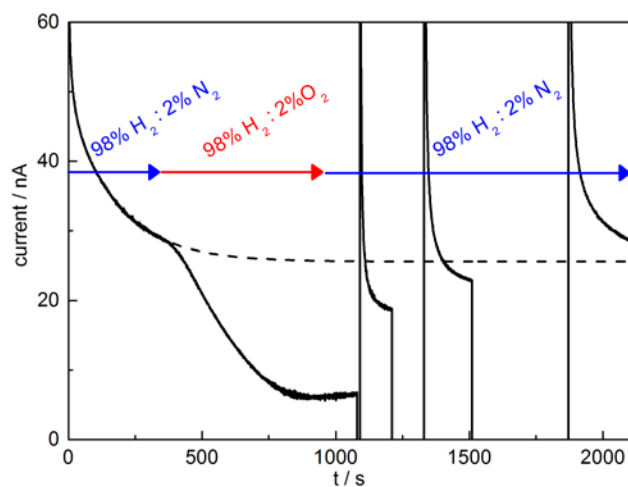


Figure 5. Current vs time trace for a pyrolytic graphite rotating disc electrode modified with RH_{stop} showing inhibition by O₂, and subsequent reductive reactivation under anaerobic conditions. The electrode was first held at +200 mV under 98% H₂ : 2% N₂. The headspace gas was exchanged during the experiment as indicated on the figure. The potential was stepped to

-400 mV at 1080 s for 1 s; at 1210 s for 120 s and at 1510 s for 300 s. Black dashed line: the exponential decay curve from the initial period at +200 mV under anaerobic conditions will have contributions from RH ‘film loss’ from the electrode, and is extrapolated to the end of the experiment. Other experimental conditions: 30 °C, the electrode was rotated at 2000 rpm throughout and the flow rate of the headgas was kept at 0.5 L min⁻¹.

Protein film infrared electrochemistry confirms that O₂ accesses the active site of RH

Infrared spectra of the active site of RH_{stop} were recorded to determine whether the effect of O₂ arises from its access to the NiFe site. Infrared spectra were recorded under 100% N₂ (Figure 6(a)i), 98% H₂, 2% N₂ (Figure 6(a)ii) and 98% H₂, 2% O₂ (Figure 6(a)iii) gas mixtures at 1 bar using protein film infrared electrochemistry (PFIRE), which combines protein film electrochemistry with ATR-IR spectroscopy. Just as in PFE the enzyme engages in direct electron transfer with a carbon electrode, and under a H₂ atmosphere the spectra reflect the steady state distribution of active site states present at each potential under catalytic turnover.⁴ Figure 6(b) shows the current recorded at an applied potential of 0 mV at the high surface area carbon particle electrode in the ATR-IR spectroelectrochemical cell during the spectroscopic experiments, with spectra collected at the times indicated. The current response is qualitatively similar to that at the PGE RDE in the first 1000 s of Figure 5, with O₂ causing a decay in electrocatalytic H₂ oxidation activity by the RH.

Figure 6(a)i shows a spectrum recorded in the absence of H₂. The spectrum is dominated by a single stretching band arising from the active site CO ligand (ν_{CO}) at 1942 cm⁻¹, characteristic of the Ni-SI_a state (Scheme 1) previously observed in the oxidized RH.³⁸ Slight asymmetry suggests

the presence of an additional active site species, and peak fitting of the ν_{CO} region indicates an additional component with a ν_{CO} band at 1938 cm^{-1} which accounts for $9\pm 2\%$ of the total recorded intensity (Supporting Information Figure S1). This minor component could correspond to a differentially protonated Ni-SI_r state of the active site.³⁹ Figure 6(a)ii shows a spectrum recorded during electrocatalytic H₂ oxidation at 0 mV. The formation of additional states of the active site in response to catalytic H₂ oxidation is clear. Two bands with ν_{CO} at 1960 cm^{-1} and a shoulder at 1943 cm^{-1} are consistent with previously observed states of the RH active site, Ni-C and Ni-SI_a, with corresponding cyanide stretching bands (ν_{CN}) at about 2072 and 2080 cm^{-1} (Supporting Information Figure S1). It has been previously reported that the ν_{CN} bands shift only slightly between the Ni-C and Ni-SI_a states of RH.^{31, 38} The ν_{CO} band at 1949 cm^{-1} , and ν_{CN} bands at 2058 and 2073 cm^{-1} (*vide infra*, Supporting Information Figure S1), are similar to those reported for the Ni-R_I state of other NiFe hydrogenases (Scheme 1).^{1, 40-41} Less intense features at 1919 , 1922 and 1934 cm^{-1} are tentatively assigned to the Ni-SI_r, Ni-R_{III} and Ni-R_{II} states, respectively, by comparison to other NiFe hydrogenases.^{1, 40-42} The ν_{CN} stretching region (Supporting Information Figure S1) contains multiple overlapping bands, consistent with the presence of several states of the RH active site. The observation of at least one Ni-R state at high potential during catalytic H₂ oxidation is significant as it reflects the involvement of Ni-R in the catalytic cycle of RH. This observation is consistent with PFIRE experiments on *E. coli* hydrogenase 1 during H₂ oxidation,⁴ and sub-turnover frequency time-resolved studies on soluble hydrogenase I from *Pyrococcus furiosus*,³ which have demonstrated the catalytic competency of the Ni-R state. In contrast to *E. coli* hydrogenase 1, however, a significant steady state concentration of Ni-SI_a ($13\pm 2\%$ of the RH_{stop} sample as determined by peak fitting, Supporting Information Figure S1) is also observed during electrocatalytic H₂ oxidation by

RH_{stop}. This indicates a slower rate of reaction of Ni-SI_a with H₂ in the case of the RH and would be consistent with restricted diffusion of H₂ into the active site, in line with some degree of gating of gas diffusion by bulky amino acid residues close to the NiFe center.

The fact that the Ni-R state has not previously been identified for *R. eutropha* RH is consistent with the observation that this enzyme has an unusually low potential proximal 4Fe4S cluster (indicated by the fact that the cluster is not reduced under a H₂ atmosphere).⁴³⁻⁴⁴ In other NiFe hydrogenases, the potential for the Ni-C/Ni-R transition appears to be similar to, or more negative than, the proximal cluster potential.¹

Figure 6(a)iii shows a spectrum recorded during inhibition of electrocatalytic H₂ oxidation in the presence of 98% H₂, 2% O₂, still at 0 mV. Under these conditions the relative intensities of the 1943 and 1960 cm⁻¹ ν_{CO} bands is reversed, and additional ν_{CO} bands are observed indicating formation of further states of the active site. Importantly, these include intense bands at 1957 and 1951 cm⁻¹, which are at similar positions to those observed for a range of inactive states in other hydrogenases, Ni-SU, Ni-B and Ni-A.^{1, 40}

Following addition of O₂ during the spectroelectrochemical PFIRE measurement the electrocatalytic current drops by about 40% (Figure 6b). This is consistent with peak fitting of the spectra shown in Figure 6(a)ii and 6(a)iii (Supporting Information Figure S1) which shows a 35% decrease in total population of ‘active’ species, Ni-C and Ni-R, and a concomitant increase in total population of ‘inactive’ species, tentatively assigned to Ni-SU, Ni-B, Ni-A and Ni-SI_r states. This provides additional support for our assignment of Ni-R, and its catalytic relevance. Similar ν_{CO} features to those we assign to inactive species were also observed in spectra of aerobically-isolated, oxidised variants of the RH that could not be reduced by H₂ despite the fact

that they displayed near-native *para/ortho*-H₂ interconversion.²² These data provide strong evidence that inhibitory O₂ interacts with the active site of the RH, showing that constriction near the active site does not completely block access to gas molecules of the size of O₂.

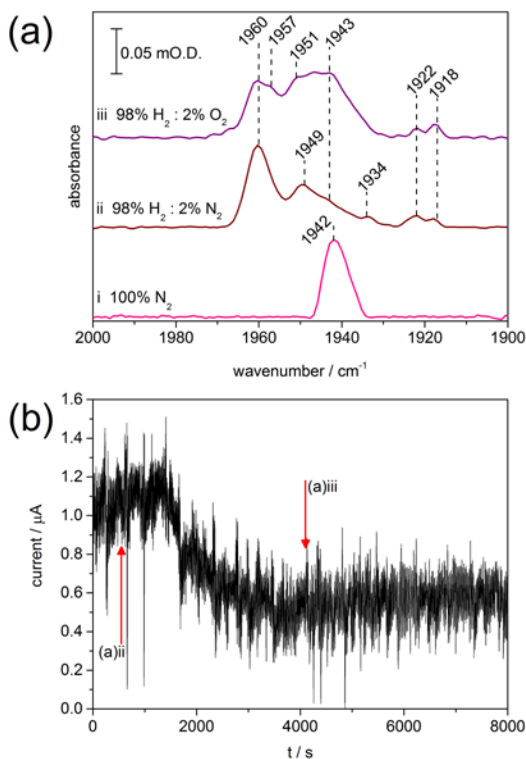


Figure 6. (a) PFIRE spectra of RH_{stop} on a carbon black electrode exposed to solution flow (20 mL min⁻¹), recorded at 0 mV in solutions saturated with (i) N₂; (ii) 98% H₂, 2% N₂ and (iii) 98% H₂, 2% O₂. The corresponding current-time trace showing inhibition of electrocatalytic H₂ oxidation is shown in (b): spectra shown in (a)ii and (a)iii were recorded at the times indicated.

Additional evidence for the assignment of bands observed during PFIRE measurements to equilibrium states of the RH active site was provided by solution phase IR spectra recorded

during slow aerobic re-oxidation of a sample of wild type RH that had been reduced by H_2 . Figure 7(a) shows a series of absorbance spectra recorded during the re-oxidation process at pH 8.0. The spectra are dominated by contributions from the Ni-C state in the most reduced samples (ν_{CO} at 1961 cm^{-1} and ν_{CN} at 2071 and 2083 cm^{-1}) and the Ni-SI_a state in the most oxidized samples (ν_{CO} at 1943 cm^{-1} and ν_{CN} at 2072 and 2081 cm^{-1}). The presence of other species can be inferred, however, by the presence of additional ν_{CO} bands during all stages of the reoxidation process.

Figure 7(b) shows difference spectra calculated from the absorbance spectra in Figure 7(a) as indicated. These difference spectra highlight the transformation of more reduced states (negative bands) to more oxidized states (positive bands) of the RH active site. Initially the Ni-C concentration increases (Figure 7(b)i), accompanied by loss of two species with ν_{CO} bands at 1935 and 1948 cm^{-1} . We therefore assign these to two of the most reduced states of the active site (Ni-R, Scheme 1), one of which (presumably the more intense 1948 cm^{-1} species) has associated ν_{CN} bands at 2058 and 2073 cm^{-1} . A small positive band at 1941 cm^{-1} in Figure 7(b)i is indicative of early Ni-SI_a formation. At intermediate times during re-oxidation (Figure 7(b)ii) most of the RH has converted to the Ni-SI_a state. In addition to reflecting the well-known redox equilibrium between Ni-C and Ni-SI_a, Figure 7(b)ii exhibits an additional positive ν_{CO} band at 1931 cm^{-1} . This indicates the formation of another oxidized species at the Ni-SI redox level, possibly Ni-SI_r. Figure 7(b)iii shows that the RH active site continues to become more oxidized at very long times, revealing a depopulation of both Ni-SI species in favor of two redox states with ν_{CO} at 1951 and 1965 cm^{-1} , possibly at the Ni-B redox level (Scheme 1). Similar higher wavenumber features were also evident in the PFIRE data (Figure 6(a)iii). The species observed during slow oxidation of the wild type RH by O_2 are consistent with those observed in the RH_{stop}

measured during electrocatalytic H₂ oxidation and following inhibition by O₂, confirming that immobilisation on an electrode does not significantly change the properties of the RH active site.

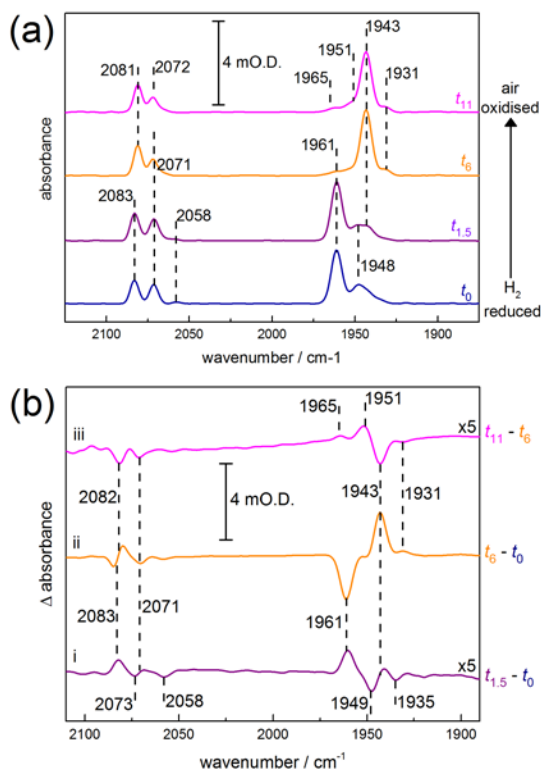


Figure 7. Aerobic oxidation of H₂-reduced wild type RH as monitored by transmission IR spectroscopy. (a) The ν_{CO} and ν_{CN} stretching regions of absorbance spectra recorded after 0.5 hours of anaerobic incubation with H₂ (blue, t_0), and after 1.5 (purple, $t_{1.5}$), 6 (orange, t_6) and 11 (magenta, t_{11}) hours of subsequent exposure to air. (b) Difference spectra calculated from the absorbance spectra in (a), relative to the H₂-reduced RH (i, $t_{1.5} - t_0$; ii, $t_6 - t_0$) and to the maximum concentration of Ni-SI_a (iii, $t_{11} - t_6$); negative and positive bands represent the depopulation of reduced states and the formation of oxidized states, respectively. Absorbance spectra were baseline corrected, while difference spectra were calculated from un-processed

single channel spectra. Spectra are offset for clarity; spectra (b)i and (b)iii were magnified by a factor of 5.

Conclusions

Regulatory NiFe hydrogenases have been considered to be distinct from other NiFe hydrogenases in their apparent insensitivity to O₂. The data from sensitive electrochemical experiments presented here show that H₂ oxidation activity of the RH from *R. eutropha* is susceptible to O₂ inactivation. Further evidence that gases larger than H₂ can inhibit the enzyme is provided by the observation that CO attenuates electrocatalytic H⁺ reduction and H₂ oxidation. Infrared spectroscopic measurements, both in solution and under turnover conditions on an electrode surface, confirm that active site states previously unreported for RH are generated in response to O₂. Notably, we have observed ν_{CO} bands at positions consistent with Ni-SU and Ni-A or Ni-B states observed in other NiFe hydrogenases. This provides strong evidence that O₂ does have an effect at the NiFe active site in the RH and therefore bulky amino acid residues near the active site do not completely block access of larger gas molecules. The observation from PFIRE spectra that Ni-SI_a is present at a significant concentration during uninhibited electrocatalytic H₂ oxidation does, however, imply that access of H₂ to the RH active site is partially restricted relative to other hydrogenases.

We have also demonstrated that RH forms at least one of the reduced, catalytically active Ni-R states following incubation under a H₂ atmosphere and in response to catalytic H₂ oxidation at high potential. Observation of the Ni-SI_a, Ni-C and Ni-R states during catalytic turnover of the RH, in line with recent studies on the NADP⁺-linked soluble hydrogenase I from *Pyrococcus*

furiosus,³ and the membrane-associated hydrogenase I from *E. coli*,⁴ indicates that the mechanism of the RH is not distinctly different from that of other classes of NiFe hydrogenases.

This study has shown that the RH from *R. eutropha* possesses rich redox chemistry and is more similar to other NiFe hydrogenases than previously appreciated.

AUTHOR INFORMATION

Corresponding Author

* kylie.vincent@chem.ox.ac.uk.

*oliver.lenz@tu-berlin.de

Author Contributions

The manuscript was written through contributions of all authors. All authors have given approval to the final version of the manuscript.

Acknowledgements

The work of K.A.V. and P.A.A. was supported by the European Research Council (EnergyBioCatalysis-ERC-2010-StG-258600), the Engineering and Physical Sciences Research Council (EP/K031503/1). Part of this research was conducted while K.A.V. was supported by a Royal Society University Research Fellowship and Research Councils UK Academic Fellowship, and collaboration between the Vincent and Lenz groups was supported by a Royal Society International Joint Project grant. We are grateful to Janna Schoknecht for purification of RH. Work of the groups of O. L. and I. Z. was supported by the Cluster of Excellence “Unifying Concepts in Catalysis” (funded by the Deutsche Forschungsgemeinschaft).

Supporting Information. Extended PFIRE data including peak fitting of the ν_{CO} region of Figure 6 and including the ν_{CN} region. This material is available free of charge via the Internet at <http://pubs.acs.org>.

ABBREVIATIONS

IR, infrared; MBH, membrane bound hydrogenase; PFE, protein film electrochemistry; PFIRE, protein film infrared electrochemistry; RH, regulatory hydrogenase; *R. eutropha*, *Ralstonia eutropha*; SH, soluble hydrogenase.

REFERENCES

1. Lubitz, W.; Ogata, H.; Rüdiger, O.; Reijerse, E., Hydrogenases. *Chem. Rev.* **2014**, *114*, 4081-4148.
2. Tai, H.; Nishikawa, K.; Suzuki, M.; Higuchi, Y.; Hirota, S., Control of the Transition between Ni-C and Ni-SI_a States by the Redox State of the Proximal Fe-S Cluster in the Catalytic Cycle of [NiFe] Hydrogenase. *Angew. Chem. Int. Ed.* **2014**, *53*, 13817-13820.
3. Greene, B. L.; Wu, C.-H.; McTernan, P. M.; Adams, M. W. W.; Dyer, R. B., Proton-Coupled Electron Transfer Dynamics in the Catalytic Mechanism of a [NiFe]-Hydrogenase. *J. Am. Chem. Soc.* **2015**, *137*, 4558-4566.
4. Hidalgo, R.; Ash, P. A.; Healy, A. J.; Vincent, K. A., Infrared Spectroscopy During Electrocatalytic Turnover Reveals the Ni-L Active Site State During H₂ Oxidation by a NiFe Hydrogenase. *Angew. Chem. Int. Ed.* **2015**, *54*, 7110-7113.
5. Fritsch, J.; Lenz, O.; Friedrich, B., Structure, Function and Biosynthesis of O₂-Tolerant Hydrogenases. *Nature Rev. Microbiol.* **2013**, *11*, 106-114.
6. Schäfer, C.; Friedrich, B.; Lenz, O., Novel, Oxygen-Insensitive Group 5 [NiFe]-Hydrogenase in *Ralstonia eutropha*. *Appl. Env. Microbiol.* **2013**, *79*, 5137-5145.
7. Lenz, O.; Ludwig, M.; Schubert, T.; Bürstel, I.; Ganskow, S.; Goris, T.; Schwarze, A.; Friedrich, B., H₂ Conversion in the Presence of O₂ as Performed by the Membrane-Bound [NiFe]-Hydrogenase of *Ralstonia eutropha*. *ChemPhysChem* **2010**, *11*, 1107-1119.
8. Horch, M.; Lauterbach, L.; Lenz, O.; Hildebrandt, P.; Zebger, I., NAD(H)-coupled Hydrogen Cycling - Structure-Function Relationships of Bidirectional [NiFe] Hydrogenases. *FEBS Lett.* **2012**, *586*, 545-556.
9. Lenz, O.; Lauterbach, L.; Frielingsdorf, S.; Friedrich, B., Chapter 4: Oxygen-tolerant Hydrogenases and Their Biotechnological Potential. In *Biohydrogen*, Rögner, M., Ed. De Gruyter: 2015; pp 61-96.
10. Lenz, O.; Friedrich, B., A Novel Multicomponent Regulatory System Mediates H₂ Sensing in *Alcaligenes eutrophus*. *Proc. Natl Acad. Sci. U.S.A.* **1998**, *95*, 12474-12479.
11. Kleihues, L.; Lenz, O.; Bernhard, M.; Buhrke, T.; Friedrich, B., The H₂ Sensor of *Ralstonia eutropha* Is a Member of the Subclass of Regulatory [NiFe] Hydrogenases. *J. Bacteriol.* **2000**, *182*, 2716-2724.

12. Liebgott, P.-P.; Dementin, S.; Leger, C.; Rousset, M., Towards Engineering O₂-tolerance in [Ni-Fe] Hydrogenases. *Energy Env. Sci.* **2011**, *4*, 33-41.
13. Ogata, H.; Hirota, S.; Nakahara, A.; Komori, H.; Shibata, N.; Kato, T.; Kano, K.; Higuchi, Y., Activation Process of [NiFe] Hydrogenase Elucidated by High-Resolution X-Ray Analyses: Conversion of the Ready to the Unready State. *Structure* **2005**, *13*, 1635-1642.
14. van Gastel, M.; Stein, M.; Brecht, M.; Schröder, O.; Lendzian, F.; Bittl, R.; Ogata, H.; Higuchi, Y.; Lubitz, W., A Single-Crystal ENDOR and Density Functional Theory Study of the Oxidized States of the [NiFe] Hydrogenase from *Desulfovibrio vulgaris* Miyazaki F. *J. Biol. Inorg. Chem.* **2006**, *11*, 41-51.
15. Vincent, K. A.; Parkin, A.; Armstrong, F. A., Investigating and Exploiting the Electrocatalytic Properties of Hydrogenases. *Chem. Rev.* **2007**, *107*, 4366-4413.
16. Fritsch, J.; Scheerer, P.; Frielingsdorf, S.; Kroschinsky, S.; Friedrich, B.; Lenz, O.; Spahn, C. M. T., The Crystal Structure of an Oxygen-Tolerant Hydrogenase Uncovers a Novel Iron-Sulphur Centre. *Nature* **2011**, *479*, 249-253.
17. Lauterbach, L.; Lenz, O., Catalytic Production of Hydrogen Peroxide and Water by Oxygen-Tolerant [NiFe]-Hydrogenase during H₂ Cycling in the Presence of O₂. *J. Am. Chem. Soc.* **2013**, *135*, 17897-17905.
18. Horch, M.; Lauterbach, L.; Mroginski, M. A.; Hildebrandt, P.; Lenz, O.; Zebger, I., Reversible Active Site Sulfoxxygenation Can Explain the Oxygen Tolerance of a NAD⁺-Reducing [NiFe] Hydrogenase and Its Unusual Infrared Spectroscopic Properties. *J. Am. Chem. Soc.* **2015**, *137*, 2555-2564.
19. Karstens, K.; Wahlefeld, S.; Horch, M.; Grunzel, M.; Lauterbach, L.; Lendzian, F.; Zebger, I.; Lenz, O., Impact of the Iron-Sulfur Cluster Proximal to the Active Site on the Catalytic Function of an O₂-Tolerant NAD⁺-Reducing [NiFe]-Hydrogenase. *Biochemistry* **2015**, *54*, 389-403.
20. Buhrke, T.; Lenz, O.; Krauß, N.; Friedrich, B., Oxygen Tolerance of the H₂-sensing [NiFe] Hydrogenase from *Ralstonia eutropha* H16 Is Based on Limited Access of Oxygen to the Active Site. *J. Biol. Chem.* **2005**, *280*, 23791-23796.
21. Bernhard, M.; Buhrke, T.; Bleijlevens, B.; Lacey, A. L. D.; Fernandez, V. M.; Albracht, S. P. J.; Friedrich, B., The H₂ Sensor of *Ralstonia eutropha*: Biochemical Characteristics, Spectroscopic Properties, and its Interaction with a Histidine Protein Kinase. *J. Biol. Chem.* **2001**, *276*, 15592-15597.
22. Gebler, A.; Burgdorf, T.; De Lacey, A. L.; Rüdiger, O.; Martinez-Arias, A.; Lenz, O.; Friedrich, B., Impact of Alterations Near the [NiFe] Active Site on the Function of the H₂ Sensor from *Ralstonia eutropha*. *FEBS J.* **2007**, *274*, 74-85.
23. Volbeda, A.; Montet, Y.; Vernède, X.; Hatchikian, E. C.; Fontecilla-Camps, J. C., High-Resolution Crystallographic Analysis of *Desulfovibrio fructosovorans* [NiFe] Hydrogenase. *Int. J. Hydrogen Energy* **2002**, *27*, 1449-1461.
24. Lukey, M. J.; Parkin, A.; Roessler, M. M.; Murphy, B. J.; Harmer, J.; Palmer, T.; Sargent, F.; Armstrong, F. A., How *Escherichia coli* Is Equipped to Oxidize Hydrogen under Different Redox Conditions. *J. Biol. Chem.* **2010**, *285*, 3928-3938.
25. Pandelia, M.-E.; Infossi, P.; Giudici-Orticoni, M. T.; Lubitz, W., The Oxygen-Tolerant Hydrogenase I from *Aquifex aeolicus* Weakly Interacts with Carbon Monoxide: An Electrochemical and Time-Resolved FTIR Study. *Biochemistry* **2010**, *49*, 8873-8881.

26. Vincent, K. A.; Cracknell, J. A.; Lenz, O.; Zebger, I.; Friedrich, B.; Armstrong, F. A., Electrocatalytic Hydrogen Oxidation by an Enzyme at High Carbon Monoxide or Oxygen Levels. *Proc. Natl Acad. Sci. U.S.A.* **2005**, *102*, 16951-16954.
27. Léger, C.; Bertrand, P., Direct Electrochemistry of Redox Enzymes as a Tool for Mechanistic Studies. *Chem. Rev.* **2008**, *108*, 2379-2438.
28. Armstrong, F. A.; Belsey, N. A.; Cracknell, J. A.; Goldet, G.; Parkin, A.; Reisner, E.; Vincent, K. A.; Wait, A. F., Dynamic Electrochemical Investigations of Hydrogen Oxidation and Production by Enzymes and Implications for Future Technology. *Chem. Soc. Rev.* **2009**, *38*, 36-51.
29. Horch, M.; Schoknecht, J.; Mroginski, M. A.; Lenz, O.; Hildebrandt, P.; Zebger, I., Resonance Raman Spectroscopy on [NiFe] Hydrogenase Provides Structural Insights into Catalytic Intermediates and Reactions. *J. Am. Chem. Soc.* **2014**, *136*, 9870-9873.
30. Cracknell, J. A.; Wait, A. F.; Lenz, O.; Friedrich, B.; Armstrong, F. A., A Kinetic and Thermodynamic Understanding of O₂ Tolerance in [NiFe]-Hydrogenases. *Proc. Natl Acad. Sci. U.S.A.* **2009**, *106*, 20681-20686.
31. Pierik, A. J.; Schmelz, M.; Lenz, O.; Friedrich, B.; Albracht, S. P. J., Characterization of the Active Site of a Hydrogen Sensor from *Alcaligenes eutrophus*. *FEBS Lett.* **1998**, *438*, 231-235.
32. Ludwig, M.; Cracknell, J. A.; Vincent, K. A.; Armstrong, F. A.; Lenz, O., Oxygen-tolerant H₂ Oxidation by Membrane-bound [NiFe] Hydrogenases of *Ralstonia* Species. *J. Biol. Chem.* **2009**, *284*, 465-477.
33. Schneider, K.; Schlegel, H. G., Purification and Properties of Soluble Hydrogenase from *Alcaligenes eutrophus* H 16. *Biochim. Biophys. Acta* **1976**, *452*, 66-80.
34. Ogata, H.; Mizoguchi, Y.; Mizuno, N.; Miki, K.; Adachi, S.-i.; Yasuoka, N.; Yagi, T.; Yamauchi, O.; Hirota, S.; Higuchi, Y., Structural Studies of the Carbon Monoxide Complex of [NiFe]hydrogenase from *Desulfovibrio vulgaris* Miyazaki F: Suggestion for the Initial Activation Site for Dihydrogen. *J. Am. Chem. Soc.* **2002**, *124*, 11628-11635.
35. van der Zwaan, J. W.; Albracht, S. P. J.; Fontijn, R. D.; Roelofs, Y. B. M., EPR Evidence for Direct Interaction of Carbon Monoxide with Nickel in Hydrogenase from *Chromatium vinosum*. *Biochim. Biophys. Acta* **1986**, *872*, 208-215.
36. Pandelia, M.-E.; Ogata, H.; Currell, L. J.; Flores, M.; Lubitz, W., Inhibition of the [NiFe] Hydrogenase from *Desulfovibrio vulgaris* Miyazaki F by Carbon Monoxide: An FTIR and EPR Spectroscopic Study. *Biochim. Biophys. Acta* **2010**, *1797*, 304-313.
37. Leroux, F.; Dementin, S.; Burlat, B.; Cournac, L.; Volbeda, A.; Champ, S.; Martin, L.; Guigliarelli, B.; Bertrand, P.; Fontecilla-Camps, J.; Rousset, M.; Léger, C., Experimental Approaches to Kinetics of Gas Diffusion in Hydrogenase. *Proc. Natl Acad. Sci. U.S.A.* **2008**, *105*, 11188-11193.
38. Healy, A. J.; Ash, P. A.; Lenz, O.; Vincent, K. A., Attenuated Total Reflectance Infrared Spectroelectrochemistry at a Carbon Particle Electrode; Unmediated Redox Control of a [NiFe]-Hydrogenase Solution. *Phys. Chem. Chem. Phys.* **2013**, *15*, 7055-7059.
39. Pandelia, M.-E.; Ogata, H.; Currell, L.; Flores, M.; Lubitz, W., Probing Intermediates in the Activation Cycle of [NiFe] Hydrogenase by Infrared Spectroscopy: the Ni-SI_r State and Its Light Sensitivity. *J. Biol. Inorg. Chem.* **2009**, *14*, 1227-1241.
40. Millo, D.; Pandelia, M.-E.; Utesch, T.; Wisitruangsakul, N.; Mroginski, M. A.; Lubitz, W.; Hildebrandt, P.; Zebger, I., Spectroelectrochemical Study of the [NiFe] Hydrogenase from

Desulfovibrio vulgaris Miyazaki F in Solution and Immobilized on Biocompatible Gold Surfaces. *J. Phys. Chem. B* **2009**, *113*, 15344-15351.

41. Saggu, M.; Zebger, I.; Ludwig, M.; Lenz, O.; Friedrich, B.; Hildebrandt, P.; Lenzian, F., Spectroscopic Insights into the Oxygen-tolerant Membrane-associated [NiFe] Hydrogenase of *Ralstonia eutropha* H16. *J. Biol. Chem.* **2009**, *284*, 16264-16276.

42. de Lacey, A. L.; Hatchikian, E. C.; Volbeda, A.; Frey, M.; Fontecilla-Camps, J. C.; Fernandez, V. M., Infrared-Spectroelectrochemical Characterization of the [NiFe] Hydrogenase of *Desulfovibrio gigas*. *J. Am. Chem. Soc.* **1997**, *119*, 7181-7189.

43. Shafaat, H. S.; Rüdiger, O.; Ogata, H.; Lubitz, W., [NiFe] Hydrogenases: A Common Active Site for Hydrogen Metabolism under Diverse Conditions. *Biochim. Biophys. Acta* **2013**, *1827*, 986-1002.

44. Roncaroli, F.; Bill, E.; Friedrich, B.; Lenz, O.; Lubitz, W.; Pandelia, M.-E., Cofactor Composition and Function of a H₂-Sensing Regulatory Hydrogenase as Revealed by Mossbauer and EPR Spectroscopy. *Chem. Sci.* **2015**, DOI: 10.1039/C5SC01560J.

Table of Contents Graphic:

Electrochemical and infrared spectroscopic studies of a regulatory NiFe hydrogenase reveal inhibition by CO and O₂

